frontiers in Materials

ORIGINAL RESEARCH
published: 03 March 2020
doi: 10.3389/fmats.2020.00045

Polypyrrole Modified E-Coat Paint for Corrosion Protection of Aluminum AA1200

Giseli Contri[1], Camila Aparecida Zimmermann[1], Sílvia Daniela Araújo Da Silva Ramoa[1], Débora Pereira Schmitz[1], Luiz Gustavo Ecco[1], Guilherme Mariz de Oliveira Barra[1] and Michele Fedel[2]*

[1] Department of Mechanical Engineering, Federal University of Santa Catarina, Florianópolis, Brazil, [2] Department of Industrial Engineering, University of Trento, Trento, Italy

OPEN ACCESS

Edited by:
Rani Elhajjar,
University of Wisconsin–Milwaukee,
United States

Reviewed by:
Elaine Armelin,
Universitat Politecnica de Catalunya,
Spain
Azman Hassan,
University of Technology, Malaysia,
Malaysia
Issam Qamhia,
University of Illinois
at Urbana–Champaign, United States

***Correspondence:**
Giseli Contri
giselicontri2@gmail.com

Specialty section:
This article was submitted to Polymeric and Composite Materials, a section of the journal Frontiers in Materials

Received: 22 August 2019
Accepted: 12 February 2020
Published: 03 March 2020

Citation:
Contri G, Zimmermann CA, Ramoa SDADS, Schmitz DP, Ecco LG, Barra GMO and Fedel M (2020) Polypyrrole Modified E-Coat Paint for Corrosion Protection of Aluminum AA1200. Front. Mater. 7:45. doi: 10.3389/fmats.2020.00045

This article reports the potential use of Polypyrrole (PPy) particles as anticorrosive additive on an epoxy water-based paint to increase the corrosion protective property of aluminum-coated panels. AA1200 aluminum panels were painted using the electrophoretic deposition method and the coatings with different concentrations of PPy particles were tested. PPy particles were synthetized by oxidative polymerization of pyrrole (Py) with iron (III) chloride hexahydrate ($FeCl_3.6H_2O$) in the presence of dodecylbenzenesulfonic acid (DBSA). Electrically conducting PPy particles (6.5 S cm^{-1}) were obtained with a size average of 154 nm. The as-prepared PPy particles were added into a water-based epoxy paint and AA1200 panels were coated via electrophoretic deposition method. The corrosion protective properties of e-coated AA1200 panels were evaluated by means of electrochemical impedance spectroscopy over prolonged exposure time in neutral non-aerated 0.1 M sodium chloride NaCl electrolyte. In particular, the addition of 0.4% by weight PPy has improved the coating corrosion protective property with respect to epoxy clearcoat and exhibited the highest value of impedance modulus at low frequency among the studied coatings.

Keywords: conductive polymers, electrophoretic deposition, organic coatings, EIS, Polypyrrole

INTRODUCTION

Cathodic electrodeposition of paints, also known as e-coat or cathodic painting, denotes an application paint method used to coat metals with organic coatings. In cathodic electrodeposition, water is used as dispersive medium and the formulations are heavy-metals free (Romano et al., 2011; Chimenti et al., 2017; Fedel, 2017). The water-based formulations, constituted of polymer and stabilized additives are deposited onto the surface of the cathode, i.e., metal to be coated, under the application of an electric field (Wicks et al., 1999). A variety of metals including aluminum alloys can be used as cathodes (Dalmoro et al., 2015). The cathodes are coated with a homogeneous highly adherent layer whose composition and dry film thickness are precisely controlled (usually within 10–30 μm) and with excellent resistance to corrosion (Bodo and Poth, 2012). In industry, cathodic electrodeposition has advantages of ease of automation therefore it is a cost-effective method of applying organic coatings in addition of being environmentally friendly (Krylova, 2001; García and Suay, 2009; Fedel et al., 2010; Rossi et al., 2017). The automotive industry is the biggest successful

example of cathodic electrodeposition application. The cathodic painting has been used to coat automobile bodyworks since its implementation in the 70′s and still remains widely used nowadays due to the advantages previously described (Bodo and Poth, 2012; Bučko et al., 2015). Recent studies in the use of cathodic electrodeposition have dealt with the incorporation of ceria oxide nanoparticles (Živković et al., 2014), graphene (Rossi and Calovi, 2018), SiO_2 (Abd El-Lateef and Khalaf, 2019) into the paint formulation as attempts to improve their anticorrosion properties (Bodo and Poth, 2012).

In recent years, intrinsically conducting polymers (I) have attracted attention of research groups for anticorrosion applications (Hosseini et al., 2011; Gurunathan et al., 2013; Ecco, 2014; Kamaraj et al., 2015; Aravindan and Sangaranarayanan, 2016; Qiu et al., 2017; Contri et al., 2018; Chen et al., 2019). Among them, the polypyrrole (PPy) stands out mainly because of its properties, such as: ease of synthesis, low cost, control of electrical conductivity, and high stability in environmental conditions, compared to other polymers of the same class (Ramôa et al., 2014). In addition, the PPy has the ability to change its oxidation state, depending on the characteristics of the medium. This behavior allows to create a passive layer on the surface of the metal, reduce the corrosion reaction rate and improve the corrosion protection of the metal (Castagno et al., 2011; Gergely et al., 2011; González and Saidman, 2012; Qi et al., 2015; Jiang et al., 2019). The PPy can be obtained by several techniques and one of the most used is the chemical oxidation of the pyrrole in the presence of stabilizers for the production of an aqueous dispersion (Ramôa et al., 2014). Thus, an aqueous dispersion modified epoxy resin system based on PPy in aqueous dispersion can be employed on a cathodic electrodeposition to produce a polymeric coating on a metal surface.

Many studies reported in the open literature have shown the potentiality of PPy-filled epoxy coatings in preventing for corrosion of aluminum alloys (Arenas et al., 2008; Qi et al., 2008; Yan et al., 2010; Castagno et al., 2011; Jadhav et al., 2013). Good adhesiveness on metallic substrate, suitable chemical and mechanical properties, environmental stability, excellent corrosion resistance for metallic materials and non-toxicity are among the strengths of PPy-filled epoxy coatings (Gupta et al., 2013). Jadhav et al. (2013) noted the effectiveness of PPy-filled-epoxy systems on the corrosion inhibition onto AA 2024-T3 aluminum alloy surface. They concluded that these coatings containing epoxy resin and conducting polymer present comparable electrochemical properties to hexavalent chromates. Therefore, they are promising candidates for chromates replacement (Jadhav et al., 2013). Moreover, Hosseini et al. (2011) have formulated "smart" corrosion protective PPy/Epoxy coatings on AA5000 aluminum alloy panels. These authors also demonstrated the importance of the secondary dopant for corrosion mechanism (Hosseini et al., 2011). In this work, anionic surfactant DBSA was used as the secondary dopant to improve pigment dispersibility by improving pigment wetting characteristics, preventing reaggregation, and increasing the stability of the dispersion (Tracton, 2007). DBSA also is used in the PPy synthesis acting as co-dopant improving it's electrical conductivity (Ramôa et al., 2015; Contri et al., 2018; Vargas et al., 2018). To advance knowledge on the corrosion inhibition effect of PPy as well as the viability of using PPy as anticorrosive additive for e-coat water-based formulations, this paper presents the potential of PPy particles to be used as anticorrosive additive on an epoxy water-based paint in order to increase the corrosion protective property of aluminum-coated panels. The scientific and technological contribution of this study is related to three main aspects: (i) obtaining a stable cataphoretic bath containing PPy particles; (ii) deposition of a thin film on the surface of a metal substrate by cataphoresis technique and (iii) development of a coating for corrosion protection of AA1200 H14 aluminum alloy. The obtained results are expected to provide understandings on the potential of PPy for Al corrosion inhibition as well as on the application of PPy particles as anticorrosive additive for E-coat water-based formulations.

EXPERIMENTAL

Synthesis of PPy

The used materials were: Pyrrole (Py) 98% and dodecylbenzene sulfonic acid (DBSA) purchased from Sigma Aldrich. Iron (III) chloride hexahydrate ($FeCl_3.6H_2O$) analytical grade purchased from Vetec Química Fina, Brazil. Before use, the Py has been double distilled for impurities removal and stored at 4°C while DBSA and $FeCl_3.6H_2O$ were used as received.

In a typical preparation route to obtain PPy (Ramôa et al., 2014), two aqueous solutions of 2.5 g DBSA and 0.25 mol of $FeCl_3.6H_2O$ were prepared in distilled water under mechanical stirring. $FeCl_3.6H_2O$ was selected as reaction initiator and DBSA acted as surfactant and dopant agent. The solution containing $FeCl_3.6H_2O$ was poured onto the DBSA solution under mechanical stirring. The mixture was kept under agitation for 10 min. After that, an aqueous solution of 0.11 mol of Py was poured dropwise on the previous prepared mixture under agitation. The reaction was carried out for 24 h under agitation at room temperature, 22°C. The obtained PPy particles were vacuum filtered, abundantly washed using distilled water and dried under reduced pressure at 60°C for 24 h.

PPy Particles Characterization

The mean volumetric size and size distribution of the PPy particles were evaluated using Dynamic Light Scattering (DLS) at 180° with 780 nm laser using a NANO-flex equipment from MICROTRAC EUROPE. Due to the pasty appearance of the PPy dispersion, was necessary dilute with deionized water to 6 mg mL^{-1}, to conduct the analysis. The analysis was conducted at a temperature of 21 ± 2°C, using as parameters spherical and absorptive particles in the Microtrac software 11.1.1.0.3. Readings were reported as the average of three consecutive readings calculated by the software.

The PPy particles surface zeta potential measurements, were evaluated using Microtrac Stabino® equipment from MICROTRAC EUROPE. The zeta potential obtained was directly

calculated by Stabino Particle Metrix 2.00.27.02 software. The PPy dispersion was diluted with deionized water to 6 mg. mL^{-1} at pH 5, equal to the pH of the cataphoretic bath, and the analysis conducted at a temperature of 21 ± 2°C.

Scanning electron microscopy (SEM) was used to observe the PPy particles morphology using a JEOL equipment model JSM-6390LV (JEOL, United States). Prior to the analysis, PPy powder particles were gold-coated. An accelerating voltage of 15 keV was used.

Electrical conductivity of PPy measurements were taken at room temperature using a four-probe apparatus. The electrical current was applied with a Keithley 6220 (United States) current source and the resulting voltage was registered by a Keithley Model 6517A (United States) electrometer. For sample preparation, first the powder was oven dried, and then molded to a 13 mm diameter pastille by compression molding. A Bovenau hydraulic press, model P15 ST, was used. The average of five measurements for each sample was calculated for results expression.

Aluminum alloy AA1200 panels (dimension of 75 × 35 × 1 mm) were used as substrates. **Table 1** reports the alloy composition. Before the experimental tests, the panels were immersed in acetone for 10 min in an ultrasonic bath, followed by rinsing with distilled water, soaking in 5% by weight NaOH for 6 min, rinsed again with water and let dry using compressed air. All steps were conducted at room temperature.

Coatings Preparation

The epoxy paints deposition on AA1200 substrates was conducted by electrophoretic deposition method using an epoxy-based binder supplied by Arsonsisi, Lainate, MI, Italy (Arsonkote 212). The coatings were prepared by diluting the epoxy-based binder with distilled water under mechanical stirring. The final volume was adjusted to 0.5 L. The produced and studied specimens were the epoxy clearcoat and epoxy loaded with PPy particles at 0.4%, 0.8%, and 1.2% by weight, as described in **Table 2**. The incorporation of as-prepared PPy particles was calculated considering the dissolved epoxy-based binder final weight. The epoxy clearcoat was used as the reference specimen and the variable under investigation was the concentration of PPy particles in the coating formulation. The deposition bath presented pH of 5.7, total solids content of 15.2% by weight and ionic conductivity near 1.14 mS cm^{-1}. The pH and the ionic conductivity did not change by adding the PPy particles in the cataphoretic bath.

Aluminum alloy AA1200 panels of 75 × 35 × 1 mm prepared as mentioned in the item 2.2. were used as cathodes and one AISI 316 stainless steel panel was used as the anode during coatings deposition. The ratio between the electrodes areas was 1:1. The electrodeposition on the cathodes was carried out applying 150 Volts for 120 s with a Pulsed DC Generator MKS, model RDPG 50 5KW (United States). The cataphoretic bath temperature was kept at 28°C. After the depositions, the coated aluminum panels were put at 180°C for 30 min in vacuum oven for crosslinking. The time, temperature, voltage, and pH values used during the coating procedure and crosslinking, are in accordance with the epoxy-based binder supplier's data sheet. Thickness measurements of dry film coatings were taken with an AKSO equipment, model AK157 following the ASTM D6132-13 standard (**Table 2**). **Table 2** lists the coatings identification, amount of added PPy particles and samples dry film thickness.

TABLE 1 | AA1200 H14 composition alloy as informed by the supplier.

Element	Si + Fe	Cu	Mn	Mg	Zn	Ti	Others	Al
%	0.74	0.01	0.02	0.01	0.01	0.02	0.03	99.18

TABLE 2 | Coatings identification (labels), fillings of each sample and their dry film thickness.

Label	Material	PPy into E-coat formulation (% by weight)	Dry film thickness (μm)
E-coat	Dissolved epoxy-based binder (Arsonkote 212)	–	10.7 ± 0.4
E-coat/PPy 0.4	Dissolved epoxy-based binder + PPy particles	0.4	12.4 ± 1.5
E-coat/PPy 0.8		0.8	17.0 ± 1.1
E-coat/PPy 1.2		1.2	20.0 ± 1.0

Characterization of the Coatings

The obtained coatings were evaluated by fourier-transform infrared spectroscopy (FTIR) in the range from 4000 up to 600 cm^{-1} with a step-size of 4 cm^{-1}. An infrared spectrometer Bruker Tensor 27 (Bruker, United States) with attenuated total reflection (ATR) accessory were used for spectra acquisition.

Adhesion of e-coat films was assessed via cross-cut test according to ISO 2409:2007 using Scotch fibrous tape #880 (purchased from 3M) before immersion tests. The spacing of the cuts were 2 mm. The tape was placed parallel to one cutting direction on the e-coat film, pressed for air removal and after 5 min it was pulled off. The appearance of the cross-cut site was evaluated based on coating detachment amount and classified according to the ISO 2409.

Electrochemical impedance spectroscopy (EIS) was carried out to evaluate the coatings protective properties. Single-sine EIS measurements were performed using a potentiostat combined with a frequency response analyzer (FRA) module (Autolab Metrohm PGSTAT302N). A single sine perturbation of 10 mV of amplitude (peak-to-peak) was applied on the samples based on the average open circuit potential (OCP), within the frequency range of 10^5 up to 10^{-2} Hz. An OCP reading time of 5 min and potential stabilization of dE/dt lower than 1 mV/s were set before EIS data acquisition. In a typical three-electrode arrangement, the coated AA1200 panels were used as the working electrodes with an Ag| AgCl reference electrode (+205 mV vs. SHE) and a stainless-steel ring counter electrode (21 cm^2). The coating area in contact with the electrolyte was 1 cm^2. All the measurements were conducted at 23°C using a non-aerated 0.1 M NaCl (sodium chloride) solution at a pH of 6.0 ± 0.2 as electrolyte.

RESULTS AND DISCUSSION

Characterization of PPy Particles

Figure 1 depicts the relative frequency distribution by volumetric size of PPy particles in water. A bimodal distribution is observed and can be related to the difficulty of maintaining a homogeneous PPy dispersion. The mean size of PPy particles was found to be near 154.1 nm. The zeta potential of the PPy dispersion at pH 5 was verified to be near −35 mV. This can be attributed to the presence of the DBSA's SO_3^- counter ions as the negative charge source in the diffuse layer of the particles.

Scanning electron microscopy micrograph of PPy particles is shown in **Figure 2**. The PPy in dry powder form is composed of agglomerates particles of different sizes and irregular shapes (Saremi and Yeganeh, 2014; Mert, 2016). Some aggregates are observed, probably responsible by the larger size particles detected in the particle size analysis. The observed particles are not perfectly spherical, due to the not formation of micelles surrounded by monomer during pyrrole polymerization (Aldissi and Armes, 1991; Boeva and Sergeyev, 2014; Vargas et al., 2018).

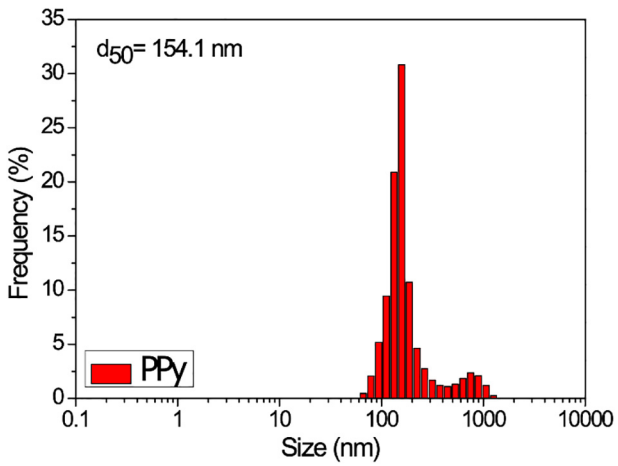

FIGURE 1 | Particle size distribution of PPy.

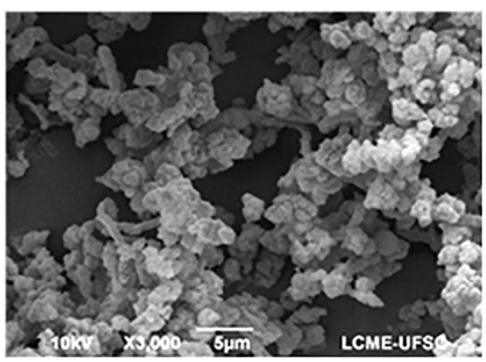

FIGURE 2 | SEM micrograph of PPy.

The PPy particles showed d.c. electrical conductivity average of 6.5 S cm^{-1}.

Characterization of the Coatings

The infrared spectra of neat e-coat, e-coat/PPy filled with 0.4%, 0.8%, and 1.2% by weight of conductive filler are depicted in **Figure 3**. The absorption band of neat e-coat in 3697 cm^{-1} is assigned to the N-H group of the primary amide of polyurethane present in the epoxy-based coating formulation, according to the product technical data sheet. The absorption band at 3361 cm^{-1} can be attributed to the hydroxyl/amine group of hydrogen bonds. Absorption bands at 2975, 2934, and 2855 cm^{-1} are attributed to the C-H stretch of aliphatic chain. In addition, the stretching vibrations of the carbonyl group urethane are observed in the absorption band at 1724 cm^{-1}. The bands at 1646 and 1609 cm^{-1} are assigned to the NH_2 group while at 1507 cm^{-1} the NH stretch of the benzene rings. The absorption band at 1226 cm^{-1} is attributed to the elongation of the vibrations of the group = C-O-C, at 913 cm^{-1} is attributed to the absorption band of the epoxy ring. And the absorption at 824 cm^{-1} attributed to the CH bonds of the aromatic ring. Similar e-coat spectra were obtained by Almeida et al. (2003), Reichinger et al. (2017) and confirm the epoxy nature of the cataphoretic coating. The spectra of coatings containing conductive additive show absorption bands overlapping on the neat e-coat.

The band at 3361 cm^{-1}, **Figure 4A**, is related to the bonded OH or NH group, a displacement to 3324 cm^{-1} for e-coat/PPy 0.4% by weight and to 3294 cm^{-1} for e-coat/PPy 0.8% and 1.2% by weight. According to Petrovic and Ferguson (1991), the frequency of hydrogen bonds changes with the strength of bonds, stronger bonds are displaced to larger wave numbers. Possibly, the observed displacements are due to the intermolecular interactions (H bonds) between the PPy additive and the neat e-coat matrix.

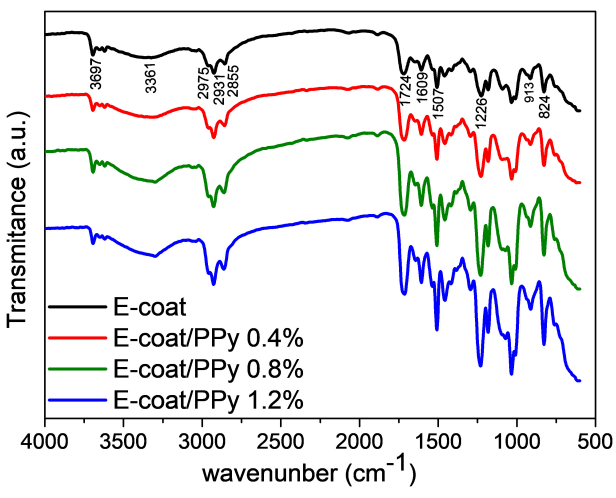

FIGURE 3 | FTIR-ATR spectrum of panels of AA1200 coated with neat e-coat and e-coat/PPy 0.4%, 0.8%, and 1.2% by weight.

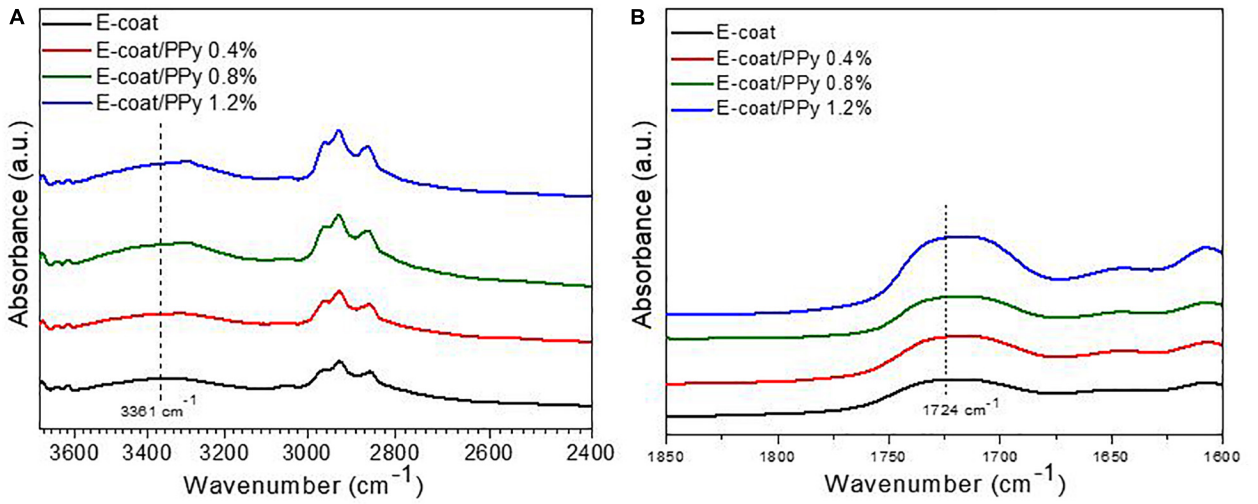

FIGURE 4 | Infrared spectra for the neat e-coat and e-coat containing 0.4%, 0.8%, and 1.2% by weight of PPy in the stretched region of the bound OH or NH **(A)** and the carbonyl stretching region **(B)**.

From **Figure 4B**, a shift in the absorption bands associated with the hydrogen bonded carbonyl group at 1724 cm^{-1} of the neat e-coat is observed for smaller values (1720, 1722, and 1721 cm^{-1}), with the addition of PPy, at respective concentrations of 0.4%, 0.8%, 1.2% by weight. This result indicates the occurrence of a higher number of hydrogen bonds between the C = O and the -NH of the urethane and/or -NH of the PPy.

Adhesion Test

The adhesion of neat e-coat and e-coats containing 0.4%, 0.8%, and 1.2% by weight of PPy was assessed using a tape peel-test, according to ISO 2409:2007, before immersion tests. All coatings were classified as grade 0 according to the ISO standard due to the absence of coating detachment as depicted in **Figure 5**. The excellent coating adhesion on AA1200 H14 aluminum alloy, implies that the coating-substrate interface presents good mechanical stability. These results indicate a proper substrate surface preparation and that the addition of different conductive additive contents in the e-coat formulation did not affect the coating adhesion on the metal substrate.

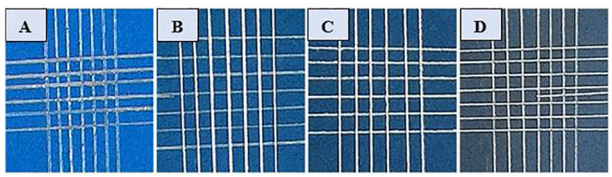

FIGURE 5 | Aspect of the samples submitted to the adhesion test of the coatings of neat e-coat **(A)**, e-coat/PPy 0.4% by weight **(B)**, 0.8% by weight **(C)**, 1.2% by weight **(D)**.

Electrochemical Tests of Coatings

Dry layer thickness is one of the most important measures for inspection and quality control of anti-corrosion coatings, which relates the barrier effect to the durability of the coating (Olajire, 2018). According to the **Table 2**, with increasing PPy concentration in the neat e-coat, the coating thickness and electrolyte permeability in the coating| metal interface increased.

Figure 6 shows the Bode diagrams of EIS spectra of the samples with neat e-coat (a1, a2), e-coat/PPy 0.4% by weight (b1, b2), e-coat/PPy 0.8% by weight (c1, c2), and e-coat/PPy 1.2% by weight (d1, d2) during 672 h immersion in chloride rich solution. In the Bode phase plot for neat e-coat, **Figure 6A1**, partially overlapping peaks indicating two-time constants are noticed. One time constant is located in 10^4–10^2 Hz and the second one in 10^1–10^{-1} Hz regarding the substrate-coating interface and the dissipative phenomena occurring in the presence of the coating, respectively. The presence of two-time constants in the e-coat/PPy 0.4% by weight appeared just within 336–672 h of exposure, which suggests an improvement in the corrosion protection of the AA1200 H14 aluminum alloy panel at this PPy load for a prolonged length of time. While the e-coat/PPy 0.8% by weight, **Figure 6C1**, and the e-coat/PPy 1.2% by weight, **Figure 6D1**, behaved similarly, with two different segments of the high and low frequency regions. These results indicate that the corrosion protection at both PPy contents (0.8% and 1.2% by weight) was not improved, since they have phase angles near to the neat e-coat. Similar results to these described above were found for Jadhav et al. (2013), Živković et al. (2015), Mert (2016), Kumar et al. (2017).

The total impedance modulus of the neat e-coat at low frequency range ($|Z|_{0.01\ Hz}$) was 10^6 Ohm cm^2 within the first 24 h of exposure (**Figure 6A2**). After 24 h, $|Z|_{0.01\ Hz}$ decreased with exposure time indicating a gradual reduction of the coating barrier effect until reaching 10^5 Ohm cm^2 at 168 h of immersion and remaining in this impedance range up to the end of the test.

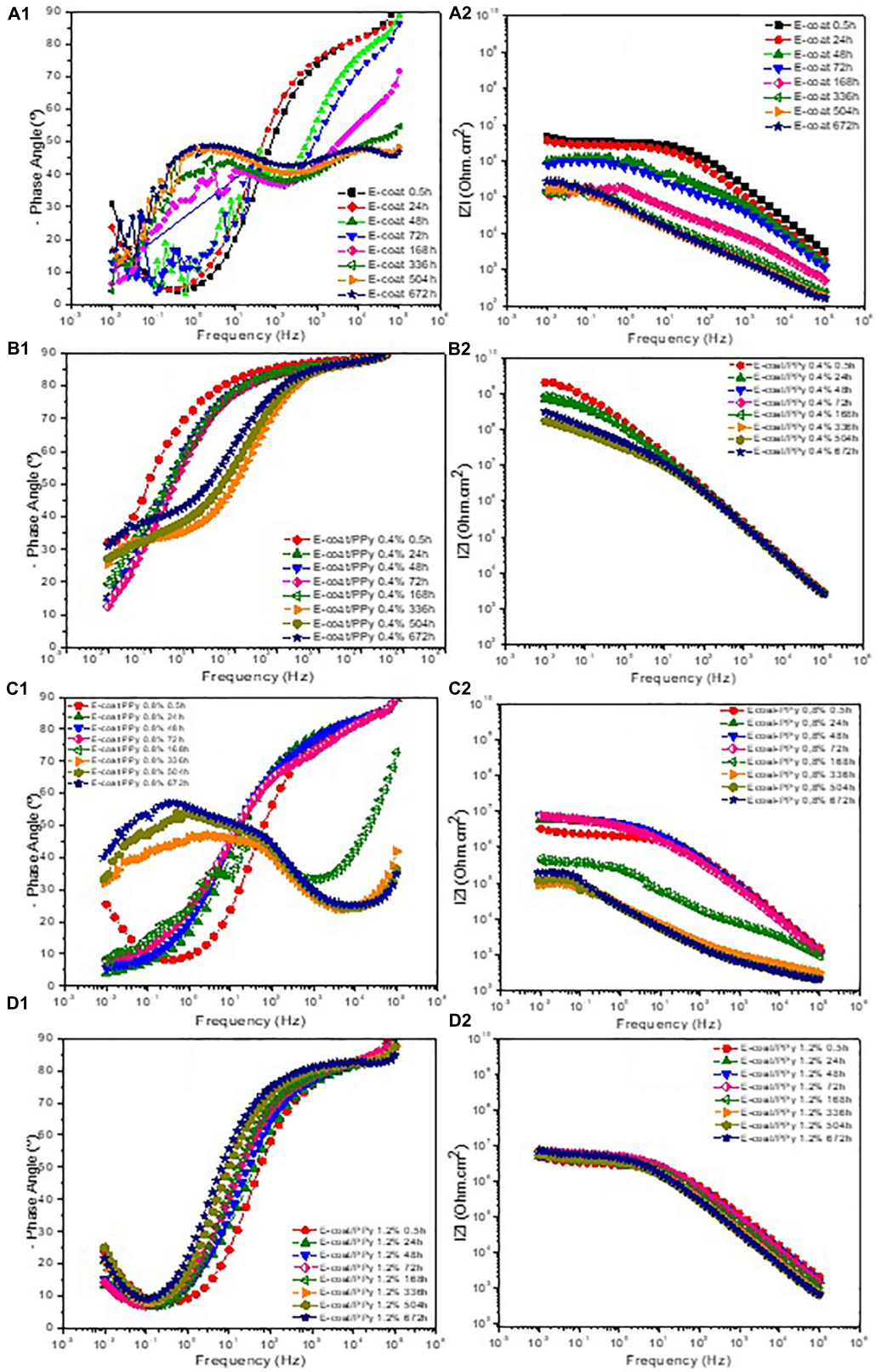

FIGURE 6 | Bode diagram for neat e-coat **(A1,A2)**, e-coat/PPy 0.4% by weight **(B1,B2)**, e-coat/PPy 0.8% by weight **(C1,C2)**, and e-coat/PPy 1.2% by weight **(D1,D2)** during 672 h exposure.

The e-coat/PPy 0.4% by weight, **Figure 6B2**, shown values of $|Z|_{0.01\ Hz}$ at 10^9 Ohm cm^2 in the first 24 h of immersion test decreasing up to 10^8 Ohm cm^2 at the end of exposure time to the electrolyte. Whereas the e-coat/PPy 0.8% by weight, **Figure 6C2**, behaved similarly to the neat e-coat. And the e-coat/PPy 1.2% by weight, **Figure 6D2**, increased by only one order of magnitude (10^7 Ohm cm^2) when compared to the neat e-coat, remaining in this impedance range without further protection improvement.

It can be concluded that the addition of PPy in the cataphoretic bath above an optimal concentration presented a detrimental effect. Instead of increasing the corrosion protection compared to the neat e-coat. This behavior can be attributed to an increased porosity allowing the free migration of the electrolyte through the coating (Bandeira et al., 2017). In this work the probable optimal concentration of PPy particles is below 0.8% by weight once the e-coat/PPy 0.4% by weight coating offered much higher impedance moduli compared to neat e-coat, that means an improved barrier effect (Huerta-Vilca et al., 2004; Contri et al., 2018).

The electrical parameters have been extracted after modeling the EIS data and the electrical equivalent circuit presented in **Figure 7**. In the equivalent circuit shown in **Figure 7A**, R_s is the electrolyte resistance, R_c the coating resistance and Q_c the constant phase element (CPE) of the coating, related to the coating capacitance. A CPE replaced the pure capacitance since the use of a CPE element with exponent *n* gives a better fitting of the spectra. The **Figure 7B** shows two-time phase constant, where R_{ct} is the resistance associated with the transfer of charges between the electrolyte and the surface of Al and the resistance associated with the passive film, Q_{dl} is the dielectric contribution of the electric double layer generated at the Al electrolyte/surface interface and the passive oxide film. Over immersion time, the electrolyte reaches the metal, resulting in two-time phase constants associated responses of oxides/hydroxides present in the metal/coating interface (Kumar et al., 2017).

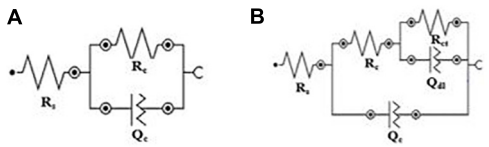

FIGURE 7 | Electrical circuits used for fitting the coatings electrical parameters. **(A)** One-time constant $R_s(Q_cR_c)$ and **(B)** two-time constants $R_s\{Q_c[R_c(Q_{dl}R_c)]\}$.

The stack plot given in **Figure 8** shows the evolution, as function of time, of the electrical parameters R_c as well as the pre-factor "Y_0" and the exponent "n" of the CPE labeled Q_{sl} + ox ($Z_{CPE} = [Y_0(\omega j)^n)]^{-1}$). R_c and Q_c values were taken into account to evaluate the level of defects in the obtained coatings (**Figures 8A,B**). The graph in **Figure 8A** shows a significant decrease in R_c value after 24 h of testing due to water absorption in the coating at the beginning of the test. Again, the sample e-coat/PPy 0.4% by weight shows a superior behavior, with resistance values always higher than 10^6 **Ω** cm^2. The other samples (neat e-coat, e-coat/PPy 0.8% and 1.2% by weight) presented a poorer performance attributed to a higher coating porosity due to conductive additive concentration bigger than an optimal content losing of the barrier effect.

The graph of **Figure 8B** shows the evolution of Q_c in the time of exposure. The pre-factor of the CPE showed a continuous reduction of its magnitudes during the period of testing. The behavior for e-coat/PPy 0.8% and 1.2% by weight were similar the neat e-coat. As a consequence, e-coat/PPy 0.8% and 1.2% by weight samples exhibited higher capacitance values by increasing the absorption of electroactive species with the time of exposure. However, it is observed for the e-coat/PPy 0.4% by weight that the capacitance values are smaller in comparison to the other coatings, indicating low water absorption by the film and presenting elevated barrier effect over time (Zanella et al., 2014).

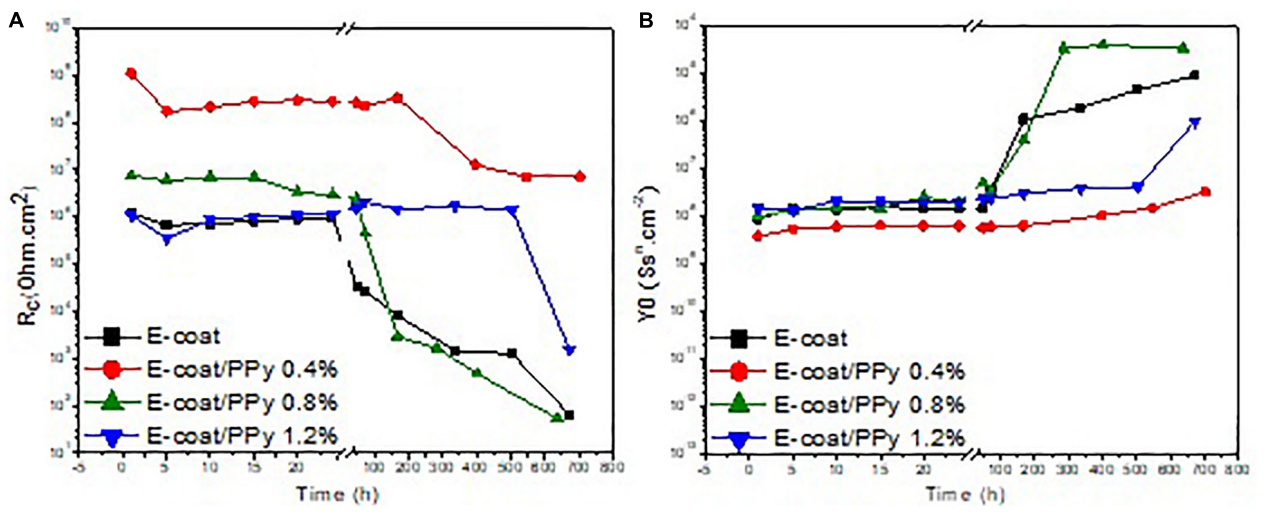

FIGURE 8 | Electrical parameters evolution **(A)** R_c and **(B)** Q_c over time for the AA1200 coated with neat e-coat and e-coat/PPy 0.4%, 0.8%, and 1.2% by weight.

CONCLUSION

In this study, a new coating for corrosion application of the AA1200 H14 aluminum alloy was successfully obtained from epoxy resin (e-coat) and PPy by the cataphoresis technique. According to the results presented in this work, it can be concluded that the e-coat/PPy 0.4%, 0.8%, and 1.2% by weight showed shifts to lower wavelengths for the absorption bands to the bonded OH and NH groups and to the carbonyl absorption bands of the urethane group, indicating that there was interaction between the PPy and the epoxy matrix. The electrodeposited coatings presented good adhesion on AA1200 H14 aluminum alloy panels, indicating that the addition of different conductive additive contents in the e-coat formulation did not affect coating performance on adhesion to the metal substrate. The electrochemical tests showed that e-coat/PPy 0.4% by weight coating provides higher impedance modulus values when compared to neat e-coat, e-coat/PPy 0.8% and e-coat/PPy 1.2% by weight.

Finally, this study showed that the coatings of e-coat/PPy are promising coatings with potential of corrosion protection for the AA1200 H14 aluminum alloy, in particular e-coat/PPy 0.4% by weight, which presented the highest anticorrosive performance during the exposure.

DATA AVAILABILITY STATEMENT

All datasets generated for this study are included in the article/supplementary material.

AUTHOR CONTRIBUTIONS

GC, CZ, LE, and SR performed the production of polymer composites composition and characterization. DS, LE, GB, and MF assisted in writing of the manuscript and discussion of the results. All authors reviewed the final manuscript.

FUNDING

This work was supported by the CNPq (Conselho Nacional de Desenvolvimento Científico e Tecnológico), the CAPES (Coordenação de Aperfeiçoamento de Pessoal de Ensino Superior), and the FAPESC (Fundação de Amparo à Pesquisa e Inovação do Estado de Santa Catarina). The Authors are grateful to Central Electronic Microscopy Laboratory (LCME-UFSC) for FESEM analyses, and Linden for particle size and zeta potential analyses.

REFERENCES

Abd El-Lateef, H. M., and Khalaf, M. M. (2019). Novel dispersed Tl_2O_3-SiO_2/polyaniline nanocomposites: in-situ polymerization, characterization and enforcement as a corrosion protective layer for carbon-steel in acidic chloride medium. *Colloids Surf. A Physicochem. Eng. Asp.* 573, 95–111. doi: 10.1016/j.colsurfa.2019.04.059

Aldissi, M., and Armes, S. P. (1991). Colloidal dispersions of conducting polymers. *Prog. Org. Coat.* 19, 21–58. doi: 10.1016/0033-0655(91)80009-8

Almeida, E., Alves, I., Brites, C., and Fedrizzi, L. (2003). Cataphoretic and autophoretic automotive primers: a comparative study. *Prog. Org. Coat.* 46, 8–20. doi: 10.1016/S0300-9440(02)00144-3

Aravindan, N., and Sangaranarayanan, M. V. (2016). Influence of solvent composition on the anti-corrosion performance of copper-polypyrrole (Cu-PPy) coated 304 stainless steel. *Prog. Org. Coat.* 95, 38–45. doi: 10.1016/j.porgcoat.2016.02.008

Arenas, M. A., Gónzalez, B. L., de Damborenea, J. J., and Ocón, P. (2008). Synthesis and electrochemical evaluation of polypyrrole coatings electrodeposited onto AA-2024 alloy. *Prog. Org. Coat.* 62, 79–86. doi: 10.1016/j.porgcoat.2007.09.019

Bandeira, R. M., Drunen, J. V., Garcia, A. C., and Tremiliosi, G. F. (2017). Influence of the thickness and roughness of polyaniline coatings on corrosion protection of AA7075 aluminum alloy. *Electrochim. Acta* 240, 215–224. doi: 10.1016/j.electacta.2017.04.083

Bodo, M., and Poth, U. (2012). *Coatings Formulation: An International Textbook*. Hanover: Vincentz Network, 288.

Boeva, Z. A., and Sergeyev, V. G. (2014). Polyaniline: synthesis, properties, and application. *Polym. Sci. Ser. C* 56, 144–153. doi: 10.1134/s1811238214010032

Bučko, M., Mišković-Stanković, V., Rogan, J., and Bajat, J. B. (2015). The protective properties of epoxy coating electrodeposited on Zn-Mn alloy substrate. *Prog. Org. Coat.* 79, 8–16. doi: 10.1016/j.porgcoat.2014.10.010

Castagno, K. R. L., Dalmoro, V., and Azambuja, D. S. (2011). Characterization and corrosion of polypyrrole/sodium dodecylbenzene sulfonate electropolymerised on aluminum alloy 1100. *Mater. Chem. Phys.* 130, 721–726. doi: 10.1016/j.matchemphys.2011.07.052

Chen, Z., Yang, W., Xu, B., Chen, Y., Qian, M., Su, X., et al. (2019). Corrosion protection of carbon steels by electrochemically synthesized V-TiO2/polypyrrole composite coatings in 0.1M HCl solution. *J. Alloys Compd.* 771, 857–868. doi: 10.1016/j.jallcom.2018.09.003

Chimenti, S., Vega, J. M., Aguirre, M., Lecina, E. G., Díez, J. A., Grande, H. J., et al. (2017). Effective Incorporation of ZnO nanoparticles by miniemulsion polymerization in waterborne binders for steel corrosion protection. *J. Coat. Technol. Res.* 14, 829–839. doi: 10.1007/s11998-017-9958-x

Contri, G., Barra, G. M. O., Ramoa, S. D. A. S., Merlini, C., Ecco, L. G., Souza, F. S., et al. (2018). Epoxy coating based on montmorillonite-polypyrrole: electrical properties and prospective application on corrosion protection of steel. *Prog. Org. Coat.* 114, 201–207. doi: 10.1016/j.porgcoat.2017.10.008

Dalmoro, V., Alemán, C. A. F., dos Santos, J. H. Z., Azambuja, D. S., Armelin, A., and Armelin, E. (2015). The influence of organophosphonic acid and conducting polymer on the adhesion and protection of epoxy coating on aluminium alloy. *Prog. Org. Coat.* 88, 181–190. doi: 10.1016/j.porgcoat.2015.07.004

Ecco, L. G. (2014). *Waterborne Paint System Based on CeO2 and Polyaniline Nanoparticles for Anticorrosion Protection of Steel*. Doctorals thesis. University of Trento, Italy.

Fedel, M. (2017). Effect of Sol–Gel layers obtained from GLYMO/MTES mixtures on the delamination of a cataphoretic paint on AA1050. *J. Coat. Technol. Res.* 14, 425–435. doi: 10.1007/s11998-016-9860-y

Fedel, M., Druart, M. E., Olivier, M., Poelman, M., Deflorian, F., and Rossi, S. (2010). Compatibility between cataphoretic electro-coating and silane surface layer for the corrosion protection of galvanized steel. *Prog. Org. Coat.* 69, 118–125. doi: 10.1016/j.porgcoat.2010.04.003

García, S. J., and Suay, J. (2009). Optimization of deposition voltage of cataphoretic automotive primers assessed by EIS and AC/DC/AC. *Prog. Org. Coat.* 66, 306–313. doi: 10.1016/j.porgcoat.2009.08.012

Gergely, A., Pfeifer, E., Bertóti, I., Török, T., and Kálmán, E. (2011). Corrosion protection of cold-rolled steel by zinc-rich epoxy paint coatings loaded with nano-size alumina supported polypyrrole. *Corros. Sci.* 53, 3486–3499. doi: 10.1016/j.corsci.2011.06.014

González, M. B., and Saidman, S. B. (2012). Properties of polypyrrole electropolymerized onto steel in the presence of salicylate. *Prog. Org. Coat.* 75, 178–183. doi: 10.1016/j.porgcoat.2012.04.015

Gupta, G., Birbilis, N., Cook, B., and Khanna, S. (2013). Polyaniline-lignosulfonate / epoxy coating for corrosion protection of AA2024-T3. *Corros. Sci.* 67, 256–267. doi: 10.1016/j.corsci.2012.10.022

Gurunathan, T., Chepuri, R. K. R., Narayan, R., and Raju, K. V. S. N. (2013). Synthesis, characterization and corrosion evaluation on new cationomeric polyurethane water dispersions and their polyaniline composites. *Prog. Org. Coat.* 76, 639–647. doi: 10.1016/j.porgcoat.2012.12.009

Hosseini, M. G., Jafari, M., and Najjar, R. (2011). Effect of polypyrrole-montmorillonite nanocomposite powders addition on corrosion performance of epoxy coatings on Al 5000. *Prog. Org. Coat.* 206, 280–286. doi: 10.1016/j.surfcoat.2011.07.012

Huerta-Vilca, D., de Moraes, S. R., and de Jesus Motheo, A. (2004). Anodic treatment of aluminum in nitric acid containing aniline, previous to deposition of polyaniline and its role on corrosion. *Synth. Met.* 140, 23–27. doi: 10.1016/s0379-6779(02)01314-0

Jadhav, N., Vetter, C. A., and Gelling, V. J. (2013). The effect of polymer morphology on the performance of a corrosion inhibiting polypyrrole/aluminum flake composite pigment. *Electrochim. Acta* 102, 28–43. doi: 10.1016/j.electacta.2013.03.128

Jiang, L., Syed, J. A., Lu, H., and Meng, X. (2019). In-situ electrodeposition of conductive polypyrrole-graphene oxide composite coating for corrosion protection of 304SS bipolar plates. *J. Alloys Compd.* 770, 35–47. doi: 10.1016/j.jallcom.2018.07.277

Kamaraj, K., Devarapalli, R., Siva, T., and Sathiyanarayanan, S. (2015). Self-healing electrosynthesied polyaniline film as primer coat for AA 2024-T3. *Mater. Chem. Phys.* 153, 256–265. doi: 10.1016/j.matchemphys.2015.01.012

Krylova, I. (2001). Painting by electrodeposition on the eve of the 21st century. *Prog. Org. Coat.* 42, 119–131. doi: 10.1016/S0300-9440(01)00146-1

Kumar, A. M., Babu, R. S., Ramakrishna, S., and de Barros, A. L. F. (2017). Electrochemical synthesis and surface protection of polypyrrole-CeO2 nanocomposite coatings on AA2024 alloy. *Synth. Met.* 234, 18–28. doi: 10.1016/j.synthmet.2017.10.003

Mert, B. D. (2016). Corrosion protection of aluminum by electrochemically synthesized composite organic coating. *Corros. Sci.* 103, 88–94. doi: 10.1016/j.corsci.2015.11.008

Olajire, A. A. (2018). Recent advances on organic coating system technologies for corrosion protection of offshore metallic structures. *J. Mol. Liq.* 269, 572–606. doi: 10.1016/j.molliq.2018.08.053

Petrovic, Z. S., and Ferguson, J. (1991). Polyurethane elastomers. *Prog. Polym. Sci.* 16, 695–836. doi: 10.1016/0079-6700(91)90011-9

Qi, K., Qiu, Y., Chen, Z., and Guo, X. (2015). Corrosion of conductive polypyrrole: galvanic interactions between polypyrrole and metal substrates. *Corros. Sci.* 91, 272–280. doi: 10.1016/j.corsci.2014.11.025

Qi, X., Vetter, C., Harper, A. C., and Gelling, V. J. (2008). Electrochemical investigations into polypyrrole/aluminum flake pigmented coatings. *Prog. Org. Coat.* 63, 345–351. doi: 10.1016/j.porgcoat.2007.12.003

Qiu, S., Chen, C., Zheng, W., Li, W., Zhao, H., and Wang, L. (2017). Long-term corrosion protection of mild steel by epoxy coating containing self-doped polyaniline nanofiber. *Synth. Met.* 229, 39–46. doi: 10.1016/j.synthmet.2017.05.004

Ramôa, S. D. A. S., Barra, G. M. O., Merlini, C., Schreiner, W. H., Livi, S., and Soares, B. G. (2015). Production of montmorillonite/polypyrrole nanocomposites through in situ oxidative polymerization of pyrrole: effect of anionic and cationic surfactants on structure and properties. *Appl. Clay Sci.* 104, 160–167. doi: 10.1016/j.clay.2014.11.026

Ramôa, S. D. A. S., Merlini, C., Barra, G. M. O., and Soares, B. G. (2014). Obtenção de nanocompósitos condutores de montmorilonita/polipirrol: efeito da incorporação do surfactante na estrutura e propriedades. *Polímeros Ciênc. Tecnol.* 24, 57–62. doi: 10.4322/polimeros.2014.051

Reichinger, M., Bremser, W., and Dornbusch, M. (2017). Interface and volume transport on technical cataphoretic painting: a comparison of steel. Hot-dip galvanised steel and aluminium alloy. *Electrochim. Acta* 231, 135–152. doi: 10.1016/j.electacta.2017.02.013

Romano, A. P., Fedel, M., Deflorian, F., and Olivier, M. G. (2011). Silane sol-gel film as pretreatment for improvement of barrier properties and filiform corrosion resistance of 6016 aluminium alloy covered by cataphoretic coating. *Prog. Org. Coat.* 72, 695–702. doi: 10.1016/j.porgcoat.2011.07.012

Rossi, S., and Calovi, M. (2018). Addition of graphene oxide plates in cataphoretic deposited organic coatings. *Prog. Org. Coat.* 125, 40–47. doi: 10.1016/j.porgcoat.2018.08.023

Rossi, S., Calovi, M., and Fedel, M. (2017). Corrosion protection of aluminum foams by cataphoretic deposition of organic coatings. *Prog. Org. Coat.* 109, 144–151. doi: 10.1016/j.porgcoat.2017.04.042

Saremi, M., and Yeganeh, M. (2014). Application of mesoporous silica nanocontainers as smart host of corrosion inhibitor in polypyrrole coatings. *Corros. Sci.* 86, 159–170. doi: 10.1016/j.corsci.2014.05.007

Tracton, A. A. (2007). *Coatings Materials and Surface Coatings*. New York, NY: CRC press, 528.

Trchová, M., and Stejskal, J. (2011). Polyaniline: the infrared spectroscopy of conducting polymer nanotubes (IUPAC Technical Report)*. *Pure Appl. Chem.* 83, 1803–1817. doi: 10.1351/pac-rep-10-02-01

Vargas, P. C., Merlini, C., Ramôa, S. D. A. S., Arenhart, R., Barra, G. M. O., and Soares, B. G. (2018). Conductive composites based on polyurethane and nanostructured conductive filler of montmorillonite/polypyrrole for electromagnetic shielding applications. *Mater. Res.* 21:e2018 0014.

Wicks, Z. W., Jones, F. N., and Pappas, S. P. (1999). *Organic Coatings: Science and Technology*. New York, NY: Wiley Interscience, 630.

Yan, M., Vetter, C. A., and Gelling, V. J. (2010). Electrochemical investigations of polypyrrole aluminum flake coupling. *Electrochim. Acta* 55, 5576–5583. doi: 10.1016/j.electacta.2010.04.077

Zanella, C., Pedrotti, A., Fedel, M., and Deflorian, F. (2014). Influence of the electrochemical behavior of metal substrates on the properties of cataphoretic clearcoat. *Prog. Org. Coat.* 77, 1987–1992. doi: 10.1016/j.porgcoat.2014.06.019

Živković, L. S., Bajat, J. B., Popić, J. P., Jegdić, B. V., Stevanović, S., and Mišković-Stanković, V. B. (2015). Protective properties of cataphoretic epoxy coating on aluminium alloy AA6060 modified with electrodeposited Ce-based coatings: effect of post-treatment. *Prog. Org. Coat.* 79, 43–52. doi: 10.1016/j.porgcoat.2014.10.014

Živković, L. S., Popić, J. P., Jegdić, B. V., Dohčević-Mitrović, Z., Bajat, J. B., and Mišković-Stanković, V. B. (2014). Corrosion study of ceria coatings on AA6060 aluminum alloy obtained by cathodic electrodeposition: effect of deposition potential. *Surf. Coat. Technol.* 240, 327–335. doi: 10.1016/j.surfcoat.2013.12.048

Conflict of Interest: The authors declare that the research was conducted in the absence of any commercial or financial relationships that could be construed as a potential conflict of interest.